

A New Way to Make Waves

Jeffrey Winicour

Max-Planck-Institut für Gravitationsphysik, Albert-Einstein-Institut,

14476 Golm, Germany

and

Department of Physics and Astronomy

University of Pittsburgh, Pittsburgh, PA 15260, USA

Abstract

I describe a new algorithm for solving nonlinear wave equations. In this approach, evolution takes place on characteristic hypersurfaces. The algorithm is directly applicable to electromagnetic, Yang-Mills and gravitational fields and other systems described by second differential order hyperbolic equations. The basic ideas should also be applicable to hydrodynamics. It is an especially accurate and efficient way for simulating waves in regions where the characteristics are well behaved. A prime application of the algorithm is to Cauchy-characteristic matching, in which this new approach is matched to a standard Cauchy evolution to obtain a global solution. In a model problem of a nonlinear wave, this proves to be more accurate and efficient than any other present method of assigning Cauchy outer boundary conditions. The approach was developed to compute the gravitational wave signal produced by collisions of two black holes. An application to colliding black holes is presented.

I. INTRODUCTION

I will describe a new way to “make waves”. Wave phenomena is treated mathematically by hyperbolic equations. Einstein’s theory of general relativity is the supreme example. It treats gravity as a distortion in the geometry of space-time. Gravitational waves are ripples in the geometry which travel through space changing the shape and size of objects in their path. At this historic time, Einstein’s theory is providing the basis for a new way to observe the distant universe. A worldwide network of gravitational wave observatories is under construction. It is designed to detect the gravitational waves produced throughout the cosmos by collisions between black holes.

The new way to make waves which I will describe was developed to simulate the production of gravitational waves by using a computer to solve Einstein’s equations. But the approach applies to any wave phenomena. In order to get the fundamental ideas across, I present them in terms of very simple systems. Only near the end will I give in to the urge to tell you about the application to black holes. However, even in simple examples, the ideas are easiest to understand in terms of space-time language and pictures.

The simplest hyperbolic equation is the 1-dimensional advection equation

$$(\partial_t + c\partial_x)\Phi = 0. \quad (1.1)$$

It has the general solution $\Phi(t, x) = F(x - ct)$, which describes a wave traveling with velocity c with initial waveform $F(x)$ at $t = 0$. The curves $x = x_0 + ct$ are called the characteristics of the equation. They are the paths in space-time (worldlines) along which you must move to “ride the wave” in the sense that $\Phi = \text{const}$ along a characteristic worldline. Since F is arbitrary, we can choose $F = 0$ for $x < 0$ and $F = 1$ for $x > 0$ to obtain a wave with a shock front along the characteristic $x = ct$. In modern parlance, this shock wave carries one bit of information. It illustrates the general way information is propagated by waves along characteristics in any hyperbolic system.

The standard way to solve a hyperbolic equation such as Eq. (1.1) is by means of the Cauchy problem. One poses initial Cauchy data $\Phi(t = 0, x)$ in some spatial region Ω and then evolves the solution in time. The characteristics causally relate the initial data to a unique evolution throughout some domain of dependence $D(\Omega)$ in space-time. As a result, shock fronts, which represent a sudden signal, can only occur across characteristics. Hyperbolic equations lead to ordinary differential equations along the characteristics which govern the propagation of shock discontinuities. That makes it important for the purpose of numerical simulation to enforce the propagation along characteristics as extensively as possible. In complicated cases, where the wave velocity has functional dependence $c(\Phi, x)$ and an analytic solution is not possible, there still exists a well established theory of the general properties of hyperbolic systems based upon characteristics [1].

The method of characteristics [2] is a computational algorithm for evolving Cauchy data based upon this theory. As applied to the advection equation (1.1), the characteristic velocities are calculated at a given discretized time $t_n = n\Delta t$ and the algorithm used to determine the field at time t_{n+1} by requiring that Φ be constant along the characteristic curve from a space-time point P at time level n to point Q at time level $n + 1$, i.e.

$$\Phi_Q = \Phi_P, \quad (1.2)$$

where $x_Q = x_P + c\Delta t$. When the wave velocity is not constant in either space or time, the points P and Q along the characteristics do not in general lie exactly on spatial grid points, so that interpolations are necessary. But, because there are no sudden changes *along* characteristics (only *across* them), such interpolations give excellent accuracy by riding the wave like a surfer.

The method of characteristics for the Cauchy problem extends to the generalization of Eq. (1.1) to any symmetric hyperbolic system of first differential order equations in a multi-dimensional space with many evolution variables and with source terms for the creation of waves [2]. However, there is another classification of hyperbolic systems, which is more familiar to physicists, based upon second order differential equations whose principal part has the form

$$g^{\alpha\beta}\partial_\alpha\partial_\beta\Phi = 0, \quad (1.3)$$

where α is a space-time index, i.e. $x^\alpha = (t, x, y, z)$ for 4-dimensional space-time, and a sum over the values of the repeated indices is implied. Equation (1.3) is classified as hyperbolic

if the symmetric matrix $g^{\alpha\beta}$ has one negative eigenvalue and its remaining eigenvalues are positive. Displacements $x^\alpha \rightarrow x^\alpha + dx^\alpha$ along characteristic worldlines satisfy

$$g_{\alpha\beta} dx^\alpha dx^\beta = 0, \quad (1.4)$$

where $g_{\alpha\beta}$, called the metric tensor, is the inverse matrix to $g^{\alpha\beta}$. The simplest example is the wave equation in one spatial dimension,

$$\left[\frac{1}{c^2}\partial_t^2 - \partial_x^2\right]\Phi = 0, \quad (1.5)$$

with the displacement along the characteristics satisfying $c^2 dt^2 - dx^2 = 0$. By rewriting Eq. (1.5) in the form

$$\left(\frac{1}{c}\partial_t - \partial_x\right)\left(\frac{1}{c}\partial_t + \partial_x\right)\Phi = 0, \quad (1.6)$$

a comparison with Eq. (1.1) shows that the general solution is $\Phi(t, x) = F(x-ct) + G(x+ct)$. There are two characteristics $x = x_0 \pm ct$ through each spatial point x_0 . Information is propagated along these characteristics which now criss-cross the space-time. The conventional method of characteristics could be applied to Eq. (1.6) by the standard technique of reducing it to a coupled system of first order differential equations. But it is simpler to integrate Eq.(1.6) over a parallelogram Σ in space time whose sides are characteristics meeting at the corners P , Q , R and S . This gives the 2-dimensional version of Eq. (1.2)

$$\Phi_Q - \Phi_P + \Phi_R - \Phi_S = 0, \quad (1.7)$$

as illustrated in Fig. 1 for the case $c = 1$ where the characteristics $x = x_0 \pm t$ have 45° slope in space-time. By using Eq. (1.7), the method of characteristics can be implemented as a computational algorithm for the Cauchy evolution of Eq. (1.5) by positioning the point Q at time level $n + 1$, the points P and S at time level n and the point R at time level $n - 1$. On a (t, x) computational grid satisfying $\Delta x = c\Delta t$, the characteristics pass through diagonal grid points. The Cauchy data, for the wave equation, which consists of the initial values $\Phi(t = 0, x)$ and $\partial_t\Phi(t = 0, x)$, is used to initialize an iterative evolution scheme at time levels $n = 0$ and $n = 1$. An exceptional feature is that the one-dimensional wave equation with constant wave velocity can be evolved *without error* by using Eq. (1.7) as a finite difference equation on such a grid. For a variable velocity, the points P , Q , R and S cannot be placed exactly on the grid and interpolations are necessary.

For the wave equation in two or more spatial dimensions, the manner in which characteristics determine domains of dependence and lead to propagation equations is qualitatively the same. The major difference is that an infinite number of characteristics now pass through each point. For the 3-dimensional wave equation,

$$\left[\frac{1}{c^2}\partial_t^2 - \partial_x^2 - \partial_y^2 - \partial_z^2\right]\Phi = 0 \quad (1.8)$$

the characteristics which pass through the point (x_0, y_0, z_0) at time t_0 are straight lines which trace out an expanding spherical wavefront of radius $c(t - t_0)$ at a given time t ; or, from

a space-time point of view, these characteristics trace out the 3-dimensional characteristic cone

$$(x - x_0)^2 + (y - y_0)^2 + (z - z_0)^2 - c^2(t - t_0)^2 = 0. \quad (1.9)$$

In electrodynamics or relativity, the characteristics are light rays and this is called the light cone. I will often use that language here. The analogue in hydrodynamics is the Mach cone.

The future (past) light cone consists of the radially outward (inward) characteristics parameterized by $t > t_0$ ($t < t_0$). There is a 2-parameter set of characteristics through each point corresponding to the sphere of angular directions (θ, ϕ) at that point. This leads to some arbitrariness in formulating an evolution algorithm for Cauchy data based upon the method of characteristics. There are an infinite number of characteristics and associated propagation equations which can be used to evolve Cauchy data from time t_0 to time $t_0 + \Delta t$.

For a practical numerical scheme, it is thus necessary either to average these propagation equations appropriately over the sphere of characteristic directions at or select out some finite number of characteristics whose propagation equations comprise a nonredundant set. The latter approach has been successfully carried out by Butler [3]. For the case of plane flow of an inviscid fluid (a problem in two spatial dimensions), he formulates an algorithm based upon four “preferred” characteristics. In this problem, the geometry is further complicated because the characteristics are dynamically dependent upon the fluid variables, in contrast to the essentially time independent characteristic cones of Eq. (1.9). In the numerical scheme, the characteristics must themselves be determined by some finite difference approximation.

That summarizes the Cauchy problem and its solution by the method of characteristics.

II. CHARACTERISTIC EVOLUTION

I now present a procedure which avoids the arbitrariness and awkwardness of the method of characteristics in a 3-dimensional Cauchy evolution. It is based upon a characteristic initial value approach rather than a Cauchy approach. In order to understand the distinction, it is essential to view space-time as 4-dimensional, with initial data given on a three-dimensional hypersurface. The Cauchy approach is based upon evolution of initial data given on a spatial hypersurface in space-time, i.e. points of space at the same instant of time $t = t_0$, to data at a later time $t = t_0 + \Delta t$. In the characteristic approach, data is initially posed on an outgoing characteristic cone (light cone), which defines a hypersurface at constant retarded time $u = u_0$. Characteristic evolution then proceeds iteratively to characteristic cones $u_n = u_0 + n\Delta u$. The numerical grid is intrinsically based upon these outgoing characteristic hypersurfaces. The algorithm for evolving from retarded time u_n to u_{n+1} is based upon characteristics which are uniquely and intrinsically picked out by the geometry of the retarded time hypersurfaces.

This characteristic evolution procedure radically differs from Cauchy evolution. It uses concepts developed in the 1960’s for studies of general relativity [4,5]. These were prompted by the inability of the major mathematical tools such as Green’s functions and Fourier analysis to overcome the difficulties posed by nonlinearity of the equations and the ambiguity of the general coordinate freedom in the theory. Its success later motivated a more extensive

mathematical treatment of the characteristic initial value problem [6]. These new techniques were especially designed for investigation of gravitational waves. A computational algorithm based on this approach has been the most successful in simulating the production of gravitational waves from black holes. [7,8]

The approach has two novel ingredients:

- the use of *characteristic hypersurfaces* to formulate a characteristic initial value problem (CIVP) and
- the use of *compactification methods* to describe on a finite grid the waves propagating to infinity.

Characteristic hypersurfaces are 3-dimensional sets traced out in space-time by characteristic worldlines or, equivalently, by their wavefronts. They provide a natural coordinate system to describe waves [4]. It is very fruitful to use an initial value scheme which describes time evolution by means of the retarded time coordinate defined by characteristic hypersurfaces as a substitute for the familiar Cauchy scheme based upon constant time hypersurfaces. As will be shown, this approach uses a completely different form of the mathematical equations and the free initial data.

Compactification methods provide a rigorous description of the radiation field of a source observed in the asymptotic limit of going to infinity along a characteristic worldline. [5]. The key idea is to introduce a new coordinate which ranges over values from 0 to 1 as the actual distance from the source ranges from 0 to ∞ . The hyperbolic equations are rewritten in terms of these new coordinates. Asymptotic behavior at the “points at infinity” can then be studied in terms of the new coordinate which ranges over finite values. In this way, the concept of the radiation zone as an *asymptotic limit at infinity* is given rigorous meaning. Characteristic hypersurfaces are important here since waves travel to infinity along characteristic worldlines, not along Cauchy hypersurfaces of constant time. Even for field equations as complicated as those of general relativity, this procedure provides a finite geometrical description of waves travelling to infinity. The limit points at infinity form a boundary to the compactified space-time, which I will refer to as *radiative infinity*. At a given retarded time, this boundary has the topology of a sphere, representing a sphere of observers at infinity.

It should be emphasized that *radiative infinity* differs drastically from *spatial infinity* (the limit of going to infinity holding time constant). Early considerations of compactifying infinite space for computational purposes were discarded because they were based upon spatial infinity [9]. An attempt to cover infinite space this way by a finite grid at constant time fails in a hyperbolic problem because there is necessarily an infinite physical distance between a grid point at infinity and its neighbors. This makes it impossible on a spatial grid at fixed time to resolve radiation with finite wave length which propagates to infinity. In contrast, for a grid constructed on a characteristic hypersurface, the grid points ride the wave without noticing its finite wavelength in the approach to radiative infinity.

In terms of characteristic coordinates $u = ct - x$ and $v = ct + x$, Eq. (1.6) becomes

$$\partial_u \partial_v \Phi = 0, \tag{2.1}$$

Here $\Psi = \partial_v \Phi$ satisfies the propagation equation

$$\partial_u \Psi = 0 \quad (2.2)$$

along the characteristics in the u -direction. This is the essence of how the use of characteristic coordinates simplifies the treatment of waves.

These ideas provide the physical basis for a new computational algorithm [10]. I will illustrate how it applies to a nonlinear version of the wave equation in 3 spatial dimensions. However, this evolution algorithm can be taken over intact to other hyperbolic physical systems, including electromagnetic fields, the Yang-Mills gauge fields of elementary particle physics, as well as general relativity, because of the common mathematical structure of these theories as second differential order hyperbolic equations. Although it has not been explored how this approach might be implemented in the case of a first differential order hyperbolic system, such as hydrodynamics, the general ideas should be applicable.

III. CHARACTERISTIC INITIAL VALUE PROBLEM FOR NONLINEAR WAVES

As a simple illustration of the characteristic initial value problem, consider the nonlinear scalar wave equation (SWE) in 3-spatial dimensions, which we write in spherical polar coordinates (t, r, θ, ϕ) as

$$\left[\frac{1}{c^2} \partial_t^2 - \partial_x^2 - \partial_y^2 - \partial_z^2 \right] \Phi = \frac{1}{c^2} \partial_t^2 \Phi - \frac{1}{r} \partial_r^2 (r\Phi) + \frac{L^2 \Phi}{r^2} = S(\Phi) \quad (3.1)$$

$$r = \sqrt{(x^2 + y^2 + z^2)}, \quad (3.2)$$

where c is the wave velocity, L^2 denotes the standard angular momentum operator

$$L^2 \Phi = - \frac{\partial_\theta (\sin \theta \partial_\theta \Phi)}{\sin \theta} - \frac{\partial_\phi^2 \Phi}{\sin^2 \theta}. \quad (3.3)$$

and $S(\Phi)$ represents a nonlinear source term. Rather than using ordinary time t , characteristic evolution uses the “retarded time” coordinate $u = ct - r$. The outgoing radial characteristics are the curves of constant u , θ and ϕ . These are the curves in the r -direction, holding $u = \text{const}$, shown in the space-time Fig. 1. In (u, r, θ, ϕ) coordinates, the SWE (3.1) takes the form

$$2\partial_u \partial_r g = \partial_r^2 g - \frac{L^2 g}{r^2} + rS. \quad (3.4)$$

where $g = r\Phi$.

The striking feature about Eq.(3.4) is that it is only first differential order in *retarded time* u , unlike the more familiar form of the SWE (3.1) which is of second differential order in *time* t . When data is given on a characteristic initial hypersurface $u = u_0$, we need only specify the initial value of the field Φ , and then use Eq. (3.4) to calculate its retarded time derivative $\partial_u \Phi$ in order to evolve the initial data. This is in contrast to the conventional Cauchy scheme, where both Φ and $\partial_t \Phi$ must be supplied at initial time $t = t_0$ and Eq. (3.1) is the used to compute the second time derivative $\partial_t^2 \Phi$ in order to evolve the data.

In a computational implementation of the CIVP, rather than finite differencing Eq. (3.4) directly, it is advantageous to first convert it into an integral equation which is subsequently discretized. Using both the outgoing characteristic coordinate u and the ingoing characteristic coordinate $v = ct + r$, the SWE (3.4) takes the form

$$4\partial_u\partial_v g = -\frac{L^2 g}{r^2} + rS\left(\frac{g}{r}\right) \quad (3.5)$$

where $g = r\Phi$. In the u - v plane formed by fixing the angular coordinates (θ, ϕ) , we construct a parallelogram Σ made up of incoming and outgoing radial characteristics which intersect at vertices P, Q, R, S as depicted in Fig. 1. By integrating Eq. (3.5) over the area Σ bounded by these vertices, we may establish the identity

$$g_Q = g_P + g_S - g_R + \frac{1}{2} \int_{\Sigma} dudv \left[-\frac{L^2 g}{r^2} + rS\left(\frac{g}{r}\right) \right]. \quad (3.6)$$

This simple identity is the 3-dimensional analogue of Eq. (1.7), adapted to include a source term. It is the starting point for an evolution algorithm which incorporates the essential role that characteristics play in the SWE.

In order to study the far field wave behavior, we transform this equation to the new radial coordinate

$$x = r/(1+r), \quad 0 \leq x \leq 1. \quad (3.7)$$

This serves to map an infinite radial domain into a finite coordinate region, and assigns infinitely distant radial points to the edge of the coordinate patch (*radiative infinity*) at $x = 1$, where the radiation signal can be identified.

A. Numerical Algorithm

To develop a discrete evolution algorithm, we work on the lattice of points

$$\begin{aligned} u_n &= n\Delta u \\ x_i &= i\Delta x \\ \zeta_{j,k} &= (j + ik)\Delta\phi \end{aligned} \quad (3.8)$$

where a complex stereographic coordinate ζ is used to cover the the sphere in two patches (North and South) in order to avoid the polar singularities of the spherical coordinates (θ, ϕ) . We denote the field at these sites by

$$g_{ijk}^n = g(u_n, x_i, \zeta_{j,k}). \quad (3.9)$$

(We will generally suppress the angular indices j and k .)

With respect to the (u, x) coordinate grid, it is not possible to place the corners P, Q, R and S at grid points since the slope of the characteristics in the compactified x coordinate depends upon location. As a consequence, the field g at these points must be interpolated

from neighboring grid points. The essential feature of the placement of the parallelogram on the grid is that the sides formed by the ingoing characteristics intersect adjacent u -hypersurfaces at equal but opposite x -displacements from the neighboring grid points, as illustrated in Fig. 2. The field values at the vertices of the parallelogram are obtained by quadratic interpolation. Cancellations between the interpolation errors at the four vertices yields the accuracy

$$g_Q - g_P - g_S + g_R = G_Q - G_P - G_S + G_R + O((\Delta x)^3 \Delta u), \quad (3.10)$$

where G represents the exact analytic solution.

The integral in Eq. (3.6) can be evaluated by treating the integrand as a constant over the parallelogram, with value at the center. The radial coordinate of the point at the center is $r_c = (r_P + r_S)/2$. To compute the nonlinear term, the value of g at r_c is taken as the average $g_c = (g_P + g_S)/2$, with g_P and g_S evaluated from second-order linear interpolations over adjacent points on the grid. The angular derivatives in Eq. (3.6) are replaced with standard second-order-accurate finite difference approximations. $L^2 g$ is calculated on the grid points, and the same interpolation procedure is used to obtain the value of $L^2 g_c$. The integral term is then approximated by

$$\begin{aligned} \int_{\Sigma} [-L^2 g + r^3 S(g/r)] du dr / r^2 &= [-L^2 g_c + r_c^3 S(g_c/r_c)] \int_{\Sigma} du dr / r^2 \\ &= 2 \log\left(\frac{r_Q r_R}{r_P r_S}\right) [-L^2 g_c + r_c^3 S\left(\frac{g_c}{r_c}\right)], \end{aligned} \quad (3.11)$$

where the integrand is accurate to second order in Δx and $\Delta \phi$. The resulting finite difference equation

$$\begin{aligned} g_i^{n+1}(x_Q + x_P - x_{i-2} - x_{i-1}) &= \\ 2g_{i-1}^{n+1}(x_Q + x_P - x_{i-2} - x_i) &- g_{i-2}^{n+1}(x_Q + x_P - x_{i-1} - x_i) \\ + \{g_{i+1}^n(x_S + x_R - x_{i-1} - x_i) &- 2g_i^n(x_S + x_R - x_{i-1} - x_{i+1}) \\ + g_{i-1}^n(x_S + x_R - x_i - x_{i+1})\} &\frac{(x_S - x_R)}{(x_Q - x_P)} \\ + \int_{\Sigma} \frac{dr du}{r^2} \left[-L^2(g_c) + r_c^3 S\left(\frac{g_c}{r_c}\right) \right] &\frac{(\Delta x)^2}{(x_Q - x_P)}. \end{aligned} \quad (3.12)$$

relates values of g_i^{n+1} with values at neighboring grid points which are either earlier in retarded time ($g_{i-1}^n, g_i^n, g_{i+1}^n$), or else contemporary but located at smaller radius ($g_{i-2}^{n+1}, g_{i-1}^{n+1}$). Consequently, it is possible to move through the grid, computing g_i^{n+1} explicitly by an orderly march. This is achieved by starting at the origin at time u_{n+1} . Field values of $g = r\Phi$ vanish there. Step outward to the next radial point, using Eq. (3.12) for all angular sites on the grid, and iterate this march out to radiative infinity thus updating the characteristic cone at u_{n+1} and completing one retarded time step. This march is then iterated in retarded time.

The algorithm steps g radially outward one cell with a local error of fourth order in grid size. This leads to second order global accuracy which is confirmed by convergence tests using known analytic solutions [10]. A complete specification of the algorithm would require a description of how the startup procedure at the origin is handled and how stereographic

coordinates are used to compute angular derivatives in a smooth way. Details of the use of North and South stereographic grids are given in Ref. [11]. Physical behavior of nonlinear waves is treated in Ref. [10]. Construction of an exact nonspherical solution for an $S = \Phi^3$ self-interaction allows calibration of the algorithm in the nonlinear case where physical singularities form. The predicted second order accuracy is confirmed right up to the formation of the singularity. Other choices of nonlinear potential allow simulation of solitons.

The Courant-Friedrichs-Lewy (CFL) condition that the numerical domain of dependence contain the physical domain of dependence (determined by the characteristics) is a necessary condition for convergence of a finite difference algorithm. For a grid point at (u, r, θ) , there are three critical grid points, at $(u - \Delta u, r + \Delta r, \theta)$ and $(u - \Delta u, r - \Delta r, \theta \pm \Delta \theta)$, which must lie inside its past characteristic cone. These gives rise to the inequalities $\Delta u < 2\Delta r$ and $\Delta u < -\Delta r + (\Delta r^2 + r^2 \Delta \theta^2)^{1/2}$. At large r , the second inequality becomes $\Delta u < r\Delta \theta$ and the Courant limit on the time step is essentially the same as for a Cauchy evolution algorithm. However, near the vertex of the cone, the second inequality gives a stricter condition

$$\Delta u < K\Delta r\Delta \theta^2, \quad (3.13)$$

where the value of K depends upon the start up procedure at the vertex. For the scalar wave equation, these stability limits were confirmed by numerical experiments [10] and it was found that $K \approx 4$.

Local von Neumann stability analysis leads to no constraints on the algorithm. This may seem surprising because no analogue of a CFL condition on the time step arises. It can be understood in the following vein. The local structure of the code is implicit, since it involves 3 points at the upper time level. Implicit algorithms do not necessarily lead to a CFL condition. However, the algorithm is explicit in the way that the evolution starts up as an outward radial march from the origin. It is this startup procedure that introduces a CFL condition.

Operating within the CFL limit, the algorithm gives a stable, globally second order accurate evolution on a compactified grid [10]. (In some nonlinear applications, artificial dissipation is necessary for stability [12].) Radiative infinity behaves as a perfectly transmitting boundary so that no radiation is reflected back into the system. Numerical evolution satisfies a conservation law relating the loss of energy to the radiation flux at infinity.

That summarizes the characteristic initial value problem and its implementation as a new computational approach to simulate waves.

IV. CAUCHY-CHARACTERISTIC MATCHING

Characteristic evolution has many advantages over Cauchy evolution. Its one disadvantage is caused by the existence of either (i) caustics where neighboring characteristics focus or (ii), a milder version of this, cross-over points where two distinct characteristics collide. The vertex of the characteristic cone is a highly symmetric example of a point caustic where a complete sphere of characteristics focus. I have already discussed how a point focus gives rise to a strong limitation imposed by the CFL condition.

Cauchy-characteristic matching (CCM) is a way to avoid such limitations by combining the strong points of characteristic and Cauchy evolution in formulating a global evolu-

tion. [7,13,14] Here I illustrate the application of CCM to the nonlinear wave equation (3.1). This problem requires boundary conditions at infinity which ensure that the total energy and the energy loss due to radiation are both finite. In a 3-dimensional problem, these are the conditions responsible for the proper $1/r$ asymptotic decay of the radiation fields. However, for practical purposes, in the computational treatment of such a system by the Cauchy problem, an outer boundary is artificially established at some large but finite distance. Some condition is then imposed upon this boundary in an attempt to approximate the proper asymptotic behavior at infinity. Such an artificial boundary condition (ABC) typically causes partial reflection of the outgoing wave back into the system [9,15–17], which contaminates the accuracy of the evolution and the radiated signal. Furthermore, nonlinear wave equations often display backscattering so that it may not be correct to try to entirely eliminate incoming radiation from the numerical solution. The errors introduced by ABC's are of an analytic origin, essentially independent of the computational discretization. In general, a systematic reduction of the error can only be achieved by simultaneously refining the grid and moving the computational boundary to a larger radius, which is computationally very expensive for three-dimensional simulations. CCM provides a global solution which does not introduce error at the analytic level.

For linear wave problems, a variety of ABC's have been proposed. For recent reviews, see Ref's. [17–20]. During the last two decades, local ABC's in differential form have been extensively employed by several authors [15,16,21–25] with varying success. Some local ABC's have been derived for the linear wave equation by considering the asymptotic behavior of outgoing solutions [22]; this approach may be regarded as a generalization of the Sommerfeld outgoing radiation condition. Although such ABC's are relatively simple to implement and have a low computational cost, their final accuracy is often limited because their simplifying assumptions are rarely met in practice [18,19]. Systematic improvement of the accuracy of local ABC's can only be achieved by moving the computational boundary to a larger radius.

The disadvantages of local ABC's have led to implementation of nonlocal ABC's based on integral representations of the infinite domain problem [18,19,29]. Even for problems where the Green's function is known and easily computed, such approaches were initially dismissed as impractical [21]; however, the rapid increase in computer power has made it possible to implement nonlocal ABC's for the linear wave equation even in 3 space dimensions [26]. For a linear problem, this can yield numerical solutions which converge to the exact infinite domain problem as the grid is refined, keeping the artificial boundary at a fixed distance. However, due to nonlocality, the computational cost per time step usually grows at a higher power of grid size ($O(N^4)$ per time step in a 3-dimensional problem with $O(N^3)$ spatial grid points) than in a local approach [18,19,26], which is demanding even for today's supercomputers. Further, the applicability of current nonlocal ABC's is restricted to problems where nonlinearity may be neglected near the grid boundary [19].

To my knowledge, only a few works have been devoted to the development of ABC's for strongly nonlinear problems [18,27,28]. In practice, nonlinear problems are often treated by linearizing the governing equations in the far field, using either local or nonlocal linear ABC's [19,20]. Besides introducing an approximation at the analytical level, this procedure requires that the artificial boundary be placed sufficiently far from the strong-field region, which sharply increases the computational cost in multidimensional simulations. There seems to be no currently available ABC which is able to produce numerical solutions which

converge (as the discretization is refined) to the infinite domain exact solution of a strongly nonlinear 3-dimensional wave problem, keeping the artificial boundary at a fixed location.

For such nonlinear problems, CCM produces an accurate solution out to radiative infinity with effort $O(N^3)$ per time-step. CCM increases the total computational cost only by a factor ~ 2 with respect to a pure Cauchy algorithm with a local ABC. The use of numerical methods based upon matching a characteristic initial-value formulation and a Cauchy formulation can effectively remove the above difficulties associated with a finite computational boundary. There is no need to truncate space-time at a finite distance from the sources, since compactification of the radial coordinate makes it possible to cover the whole space-time with a finite grid. In this way, the true radiation zone signal may be computed. Although the characteristic formulation has stability limitations in interior region where the characteristic hypersurfaces can develop caustics, it proves to be both accurate and computationally efficient in the treatment of the exterior, caustic-free region.

CCM is a new approach to global numerical evolution which is free of error at the analytic level. The characteristic algorithm provides the *outer* boundary condition for the interior Cauchy evolution, while the Cauchy algorithm supplies the *inner* boundary condition for the characteristic evolution. Since CCM consists of discretizing an exact analytic treatment of the radiation from source to radiative infinity, it generates numerical solutions which converge to the exact analytic solution of the radiating system even in the presence of strong nonlinearity. Thus, any desired accuracy can be achieved by refining the grid, without moving the matching boundary. In practice, the method performs extremely well even at moderate resolutions.

A. CCM for nonlinear waves

As an illustration of the computational implementation of CCM, consider again the nonlinear 3-dimensional wave equation (3.1). For simplicity, set the velocity $c = 1$. In the standard computational implementation of the Cauchy problem for (3.1), initial data $\Phi(t_0, x, y, z)$ and $\partial_t \Phi(t_0, x, y, z)$ are assigned and evolved in a bounded spatial region, with some ABC imposed at the computational boundary. In a characteristic initial-value formulation the SWE (3.1) is reexpressed in the form of Eq. (3.4) in terms of $g = r\Phi$, using standard spherical coordinates and a retarded time coordinate $u = t - r$. The initial data $g(u_0, r, \theta, \phi)$, on an initial outgoing characteristic cone $u = u_0$ is then evolved globally out to radiative infinity.

In CCM, (3.1) is solved in an interior region $r \leq R_m$ using a Cauchy algorithm, while a characteristic algorithm solves the retarded coordinate version (3.4) for $r \geq R_m$. The matching procedures ensure that, in the continuum limit, Φ and its gradient are continuous across the interface $r = R_m$. This is a requirement for any consistent matching algorithm, since a discontinuity in the field or its gradient could act as a spurious boundary source, contaminating both the interior and exterior evolutions.

For technical simplicity, I illustrate the details of the method here for spherically symmetric waves but it has been successfully implemented in fully nonlinear 3-dimensional problems without symmetry. In a 3-dimensional problem without symmetry, the characteristic evolution is carried out on an exterior spherical grid, while the Cauchy evolution uses a Cartesian

grid covering the interior spherical region. Although a spherical grid could also be used in the interior, a Cartesian grid avoids the necessity of cumbersome numerical procedures to handle the singularity of spherical coordinates at the origin. A Cartesian discretization in the interior and a spherical discretization in the exterior are the coordinates natural to the geometries of the two regions. However, this makes the treatment of the interface somewhat involved; in particular, guaranteeing the stability of the matching algorithm requires careful attention to the details of the inter-grid matching. Nevertheless, there is a reasonably broad range of discretization parameters for which CCM is stable [30].

With the substitution $G = r\phi$ and the use of spherical coordinates, the spherically symmetric version of the SWE (3.1) reduces to the 1-dimensional wave equation

$$\partial_{tt}G = \partial_{rr}G + rS. \quad (4.1)$$

The initial Cauchy data is $G(t_0, r)$ and $\partial_t G(t_0, r)$ in the region $0 \leq r \leq R_m$. Together with the regularity condition $G(t, 0) = 0$, these data determine a unique solution in the domain of dependence D_{1-} indicated in Fig. 3. The outer boundary of the domain of dependence is the ingoing radial characteristic C_{1-} described by $r = R_m - t + t_0$. The solution cannot be constructed throughout the complete interior region $r \leq R_m$ without additional information, which can be furnished by giving the value of G on the outgoing characteristic C_{0+} described by $r = R_m + t - t_0$ (see Fig. 3). In terms of the coordinates $u = t - r$ and r , C_{0+} is described by $u = t_0 - R_m$. In these coordinates, expressing $g(u, r) = G(u + r, r)$, the spherically symmetric version of the wave equation (3.4) is

$$2\partial_{ur}g = \partial_{rr}g + rS. \quad (4.2)$$

A unique solution of (4.2) is determined by characteristic initial data consisting of the value of g on the initial outgoing characteristic C_{0+} and on the ingoing characteristic C_{1-} . These data determine the solution uniquely throughout the future of C_{1-} and C_{0+} , i.e. the region D_{1+} in Fig. 3.

The matching scheme proceeds as shown in Fig. 3. First, initial Cauchy data are evolved from t_0 to t_1 throughout the region D_{1-} , which is in its domain of dependence. Next, this induces characteristic data on C_{1-} which combined with the initial characteristic data on C_{0+} allows a characteristic evolution throughout the region D_{1+} , bounded in the future by the characteristic C_{1+} . The solution determined from this initial stage induces Cauchy data at time t_1 in the region $r \leq R_m$, inside the matching boundary. This process can then be iterated to carry out the entire future evolution of the system.

CCM is a discretized version of this scheme in which the criss-cross pattern of characteristics inside the radius R_m is at the scale of a grid spacing. The discretized evolution algorithm consists of the following steps (see Fig. 4):

Step 1. Cauchy evolution. The interior integration scheme is implemented on a uniform spatial grid $r_i = i\Delta r$ ($0 \leq i \leq M$) with outer radius $R_B = M\Delta r$. We discretize (4.1) using the standard second-order finite difference scheme

$$\frac{G_i^{n+1} - 2G_i^n + G_i^{n-1}}{(\Delta t)^2} = \frac{G_{i+1}^n - 2G_i^n + G_{i-1}^n}{(\Delta r)^2} + r_i S_i^n, \quad (4.3)$$

where $G_i^n = G(t_n, r_i)$, $S_i^n = S(t_n, r_i)$, and $t_n = t_0 + n\Delta t$. The interior evolution is initialized by evaluating G_i^0 and G_i^1 ($0 \leq i \leq M$) to second order accuracy from the Cauchy initial

data. In the n th time step, (4.3) is used to compute G_i^{m+1} , $1 \leq i \leq M$ in terms of field values G_i^{m-1} and G_i^n . The regularity of Φ at $r = 0$ implies that $G_0^n = 0$ for all n . The boundary values G_{M+1}^n which are required by (4.3) are supplied by the matching procedure (step 3).

Step 2. Characteristic evolution. The characteristic algorithm is implemented on a uniform grid based on the dimensionless compactified radial coordinate

$$\eta = 1 - \frac{1}{1 + r/R_m}, \quad \frac{1}{2} \leq \eta \leq 1 \quad (4.4)$$

so that points at radiative infinity (corresponding to $\eta = 1$) are included in the grid. In order to include one of the technical problems in matching an interior Cartesian grid to an exterior spherical grid, let there be a small gap between the outer radius R_B of the Cauchy grid and the matching radius R_m (which is also the inner radius of the characteristic grid). In 3-dimensional Cartesian-spherical matching the outermost Cauchy grid points and the innermost characteristic grid points are necessarily distinct. This is represented here by a gap $R_m - R_B = \kappa \Delta r$, where $\kappa \geq 0$ is an arbitrary parameter. The characteristic grid consists of the uniformly spaced points $\eta_\alpha = \frac{1}{2} + \alpha \Delta \eta$ ($0 \leq \alpha \leq N_\eta$), where $\Delta \eta = (2N_\eta)^{-1}$. The retarded time levels $u = u_n$ for the characteristic evolution are chosen so that $u = u_n$ intersects the time level $t = t_n$ of the Cauchy evolution at the matching radius; therefore, $u_n = t_n - R_m$ and $\Delta u = \Delta t$. We denote by g_α^n the value of g at $\eta = \eta_\alpha$, $u = u_n$. The initial characteristic data consist of g_α^0 , $0 \leq \alpha \leq N_\eta$.

In the n th iteration of the evolution, we compute the field values at the grid points with $u = u_n$ using the values of g_α^{n-1} , which are known either from initialization or from the previous iteration. As already described, this is done by the characteristic marching algorithm based on the integral identity (3.6).

At the inner boundary of the characteristic grid ($\alpha = 1$), the previous scheme must be slightly modified, since $g_{\alpha-2}^n$ is not defined. For this initial step, $PQRS$ is chosen so that $\eta_P = \eta_0$, $\eta_Q = \eta_1$, and g_R , g_S are approximated by quadratic interpolation in terms of g_0^{n-1} , g_1^{n-1} , g_2^{n-1} , which have already been computed. Besides these field values, the final evaluation of g_1^n still requires the value of g_0^n , which is supplied by the matching procedure (step 3).

Step 3. Matching. Numerous schemes are possible in the case of spherically symmetric matching. Here I describe one which is stable for a wide range of gap sizes, $0 \leq \kappa \leq 2$ and works in the more complicated situation with an interior Cartesian grid and an exterior spherical grid.

The required boundary values G_{M+1}^n and g_0^n are computed by radial interpolations at constant t , using the field values at points A , B , E , and F in Fig. 4. The first two of these field values are already known at the n th step, while the last two can be obtained by cubic radial interpolations along the previously evolved characteristics $u = u_{n-1}$ and $u = u_{n-2}$, respectively. At the initial step, point F lies on the characteristic $u = u_{-1} = -\Delta t - R_m$, which is not evolved by the algorithm; this field value is supplied along with the initial data. Once the Cauchy and characteristic boundary values are computed, a new iteration may be performed starting from Step 1 above.

Since all the interpolations employed in the matching step have fourth order error, the matching algorithm has the same second order global accuracy exhibited by the separate

Cauchy and characteristic algorithms, as confirmed by numerical tests.

In summary, CCM has been implemented and tested for nonlinear waves in 3-dimensional space. No special assumption is made about the waves crossing the computational interface $r = R_m$ and nonlinear effects in the exterior characteristic domain are automatically taken into account. In numerical experiments CCM converged to the exact solution (with the matching boundary fixed at an arbitrary position) in highly nonlinear problems. For comparison, nonlocal ABC's yielded convergent results only in linear problems. In terms of both computational cost and accuracy, CCM is a very effective way to solve the 3-dimensional wave equations, with or without a nonlinear term. It is possible to achieve convergence with an ABC by refining the grid *and simultaneously* enlarging the radius of the outer boundary. However, this is very expensive computationally, especially for small target error in the determination of the radiated signal in a 3-dimensional problems [31]. Because CCM is convergent under grid-refinement alone, for small target error its performance is significantly better than any available alternative. In strongly nonlinear problems. CCM appears to be the only available method which is able to produce numerical solutions which converge to the exact solution with a computational interface located at an arbitrary fixed position.

V. APPLICATION TO BLACK HOLES

By definition, a black hole traces out a world tube in space-time which is the boundary of what is visible to an outside observer. As a result, this worldtube is necessarily a characteristic hypersurface traced out in space-time by light rays (the characteristics of general relativity).

A mechanical analogue of a black hole can in principle be constructed by letting a reservoir of water empty through a funnel into a lower reservoir. By arranging the flow velocity in the funnel to exceed the velocity of sound in the upper reservoir, an acoustic version of a black hole results [32]. Sound waves can travel from the upper reservoir to the lower but not in the reverse direction.

The simplest example of a black hole arises in the spherically symmetric collapse of a star whose energy has been depleted to the extent that internal pressure cannot withstand gravity. A point sized black hole first forms at the center of the collapsing star, which then expands into a sphere growing with the velocity of light, thus tracing out a light cone in space-time. Normally a light cone keeps expanding forever. What makes a black hole light cone unique is that gravity halts this expansion and eventually the black hole just hovers in equilibrium at a fixed size. Each point on the spherical black hole still moves along a light ray, but the sphere of light rays is in a delicate gravitational balance between growing and shrinking.

This spherically symmetric black hole was discovered analytically by Schwarzschild as a simple solution to Einstein's equations. Unfortunately, Schwarzschild's black hole does not emit gravitational waves (just as a spherically symmetric charge distribution does not emit electromagnetic waves).

The inspiral and merger of a binary system of black holes is a powerful source of gravitational waves, which lie in the frequency band detectable by the new gravity wave observatories. The lack of symmetry necessitates a computational treatment to determine the

waveform of the radiated signal. The binary black holes trace out a characteristic hypersurface in space-time so that their simulation by characteristic evolution is a natural approach. Using a characteristic evolution algorithm similar to that which I have described here, except now applied to Einstein's equation, we have found fascinating results. The binary black holes, rather than initially forming as a point caustic in the Schwarzschild case, form as a cross-over surface where light rays collide. This cross-over surface is itself bounded by a ring of caustics which in a sense mark the merger of the two individual black holes into a single black hole. [33,34]

The individual black holes form as spheres but, as illustrated in Fig. 5, as the holes approach, their mutual gravitational tidal distortion produces sharp pincers just prior to merger. At merger, the pincers join to form a single temporarily toroidal black hole, as illustrated in Fig. 6. The inner hole of the torus subsequently closes up to produce first a single peanut shaped black hole and finally a spherical black hole. Details of this merger can be viewed at the web site <http://artemis.phyast.pitt.edu/animations>. We are now using characteristic evolution to compute the gravitational wave signal emitted in such black hole collisions in the anticipation that they will be detected by the new gravity wave observatories.

VI. ACKNOWLEDGEMENTS

I thank the Pittsburgh Supercomputing Center and NPACI for making computing time available for this research and the National Science Foundation for research support under grant NSF PHY 9510895.

REFERENCES

- [1] F. John, *Partial Differential Equations*, (Springer-Verlag (Berlin, 4th Ed. 1982).
- [2] B. Gustafsson, H.-O. Kreiss and J. Oliger, *Time Dependent Problems and Difference Methods*, (Wiley, New York, 1995).
- [3] D. S. Butler, *Proc. R. Soc. London Ser. A* **255**, 232 (1960).
- [4] H. Bondi, M.G. van der Burg, and A.W.K. Metzner, *Proc. R. Soc. London Ser. A* **270**, 103 (1962).
- [5] R. Penrose, *Phys. Rev. Lett.* **10**, 66 (1963).
- [6] F. G. Friedlander, *The wave equation on a curved space-time*, (Cambridge U.P., 1975).
- [7] J. Winicour, Living Reviews (1998), <http://www.livingreviews.org/>
- [8] R. Gómez, L. Lehner, R. Marsa, and J. Winicour, *Phys. Rev. D* **57**, 4778 (1997).
- [9] M. Israeli and S. A. Orszag, *J. Comp. Phys.*, **41**, 115 (1981).
- [10] R. Gómez, J. Winicour and R. I. Isaacson, *J. Comp. Phys.*, **98**, 11 (1992).
- [11] R. Gómez, L. Lehner, P. Papadopoulos and J. Winicour, *Class. Quantum Grav.* **14**, 977 (1997).
- [12] L. Lehner, *J. of Comp. Phys.*, **149**, N1 , 59 (1999).
- [13] N. T. Bishop, *Class. Quantum. Grav.*, **10**, 333 (1993).
- [14] N. T. Bishop, R. Gómez, P. R. Holvorcem, R. A. Matzner, P. Papadopoulos and J. Winicour, *Phys. Rev. Letters*, **76**, 333 (1996).
- [15] E. L. Lindman, *J. Comp. Phys.*, **18**, 115 (1975).
- [16] R. E. Higdon, *Math. Comp.*, **47**, 437 (1986).
- [17] R. A. Renault, *J. Comp. Phys.*, **102**, 236 (1992).
- [18] D. Givoli, *J. Comp. Phys.*, **94**, 1 (1991).
- [19] S. V. Tsynkov, “Artificial Boundary Conditions Based on the Difference Potentials Method”, *NASA Technical Memorandum No. 110265* (Langley Research Center, 1996).
- [20] V. S. Ryaben’kii, and S. V. Tsynkov, “An Application of the Difference Potentials Method to Solving External Problems in CFD”, *CFD Review*, (1996).
- [21] B. Engquist and A. Majda, *Math. Comp.*, **31**, 629 (1977).
- [22] A. Bayliss and E. Turkel, *Commun. Pure Appl. Math.*, **XXXIII**, 707 (1980).
- [23] L. N. Trefethen and L. Halpern, *Math. Comp.*, **47**, 421 (1986).
- [24] J. G. Blaschak and G. A. Kriegsmann, *J. Comp. Phys.*, **77**, 109 (1988).
- [25] H. Jiang, and Y. S. Wong, *J. Comp. Phys.*, **88**, 205 (1990).
- [26] J. de Moerloose and D. de Zutter, *IEEE Transactions on Antennas and Propagation* , **41**, 890 (1993).
- [27] K. W. Thompson, *J. Comp. Phys.*, **68**, 1 (1987).
- [28] T. M. Hagstrom and S. I. Hariharan, *Math. Comput.*, **581**,51 (1988).
- [29] L. Ting and M. J. Miksis, *J. Acoust. Soc. Amer.*, **80**, 1825 (1986)
- [30] N. T. Bishop, R. Gómez, P. R. Holvorcem, R. A. Matzner, P. Papadopoulos and J. Winicour, *J. Comp. Phys.* **136**, 140 (1997).
- [31] N. T. Bishop, R. Gómez, L. Lehner and J. Winicour, *Phys. Rev. D* **54**, 6153 (1996).
- [32] W. G. Unruh, *Phys. Rev. D* **51**, 2827 (1995).
- [33] L. Lehner, N. T. Bishop, R. Gómez, B. Szilágyi, and J. Winicour, *Phys. Rev. D* **60**, 44005 (1999).
- [34] S. Husa and J. Winicour, *Phys. Rev. D* **60**, 84019 (1999).

FIGURES

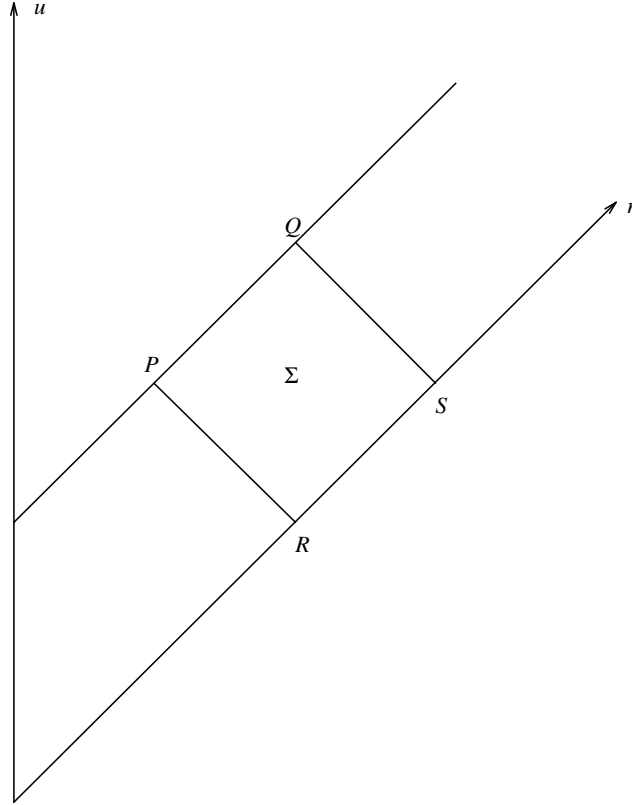


FIG. 1. Space-time picture of a parallelogram Σ formed by intersecting characteristics, where the characteristic have 45° slope. The coordinates are retarded time u and radial distance r . In standard (t, x) coordinates, the t -direction is vertical and the spatial x -direction horizontal, so that the pair P and S are at the same time t , with Q in their future and S in their past. In (u, r) coordinates, the pair P and Q are at the same retarded time, as well as the pair R and S .

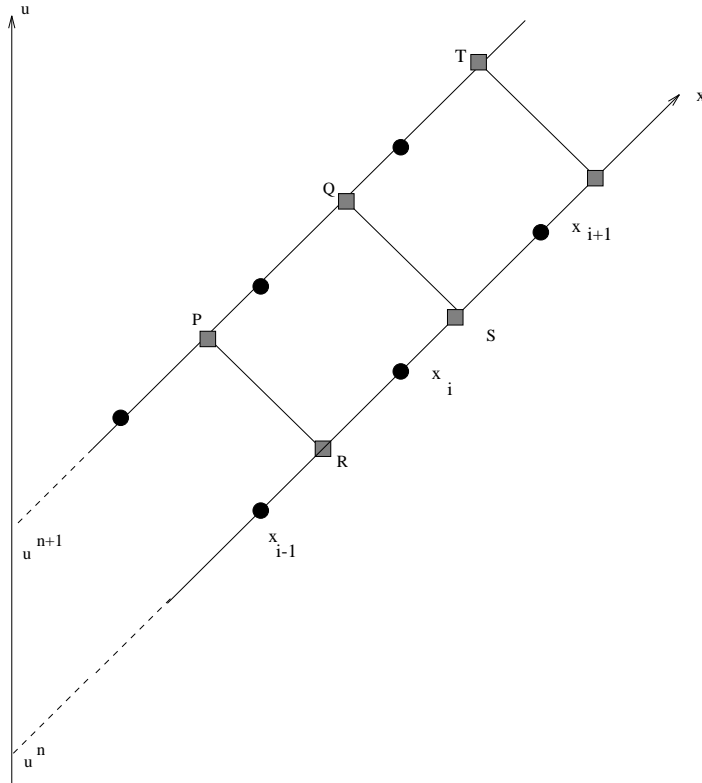


FIG. 2. Line segments drawn at forty-five degrees represent radial characteristics. Their intersection defines the fundamental null parallelogram PQRS shown superimposed upon the computational cell, which consists of the points marked by circles and their nearest neighbors in the angular directions (not shown). Here u is the retarded time coordinate and x is the compactified radial coordinate. The marching algorithm determines Φ_Q in terms of the previously determined values Φ_P , Φ_R and Φ_S . The process is then iterated to determine Φ_T on a march to radiative infinity.

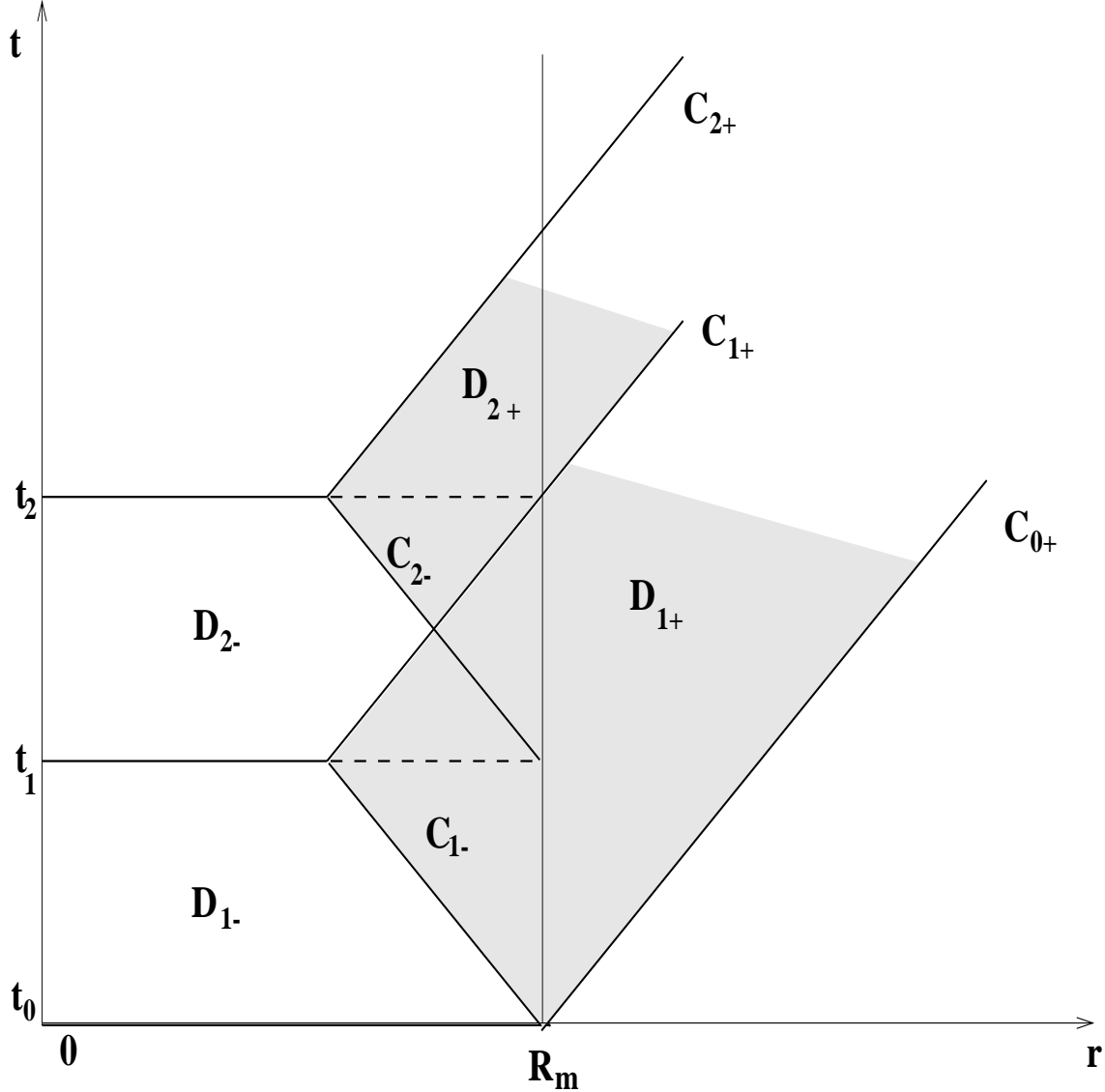


FIG. 3. Initial Cauchy data are evolved from t_0 to time t_1 throughout the region D_{1-} . Characteristic data induced on C_{1-} , combined with the initial characteristic data on C_{0+} are used to evolve the region D_{1+} . This produces Cauchy data at time t_1 in the region $r \leq R_m$. Similarly, Cauchy evolution is used in the region D_{2-} , bounded on the right by C_{2-} . The characteristic data induced on C_{2-} , together with those on C_{1+} , are sufficient to evolve through the region D_{2+} . The process can be iterated to carry out the entire future evolution of the system.

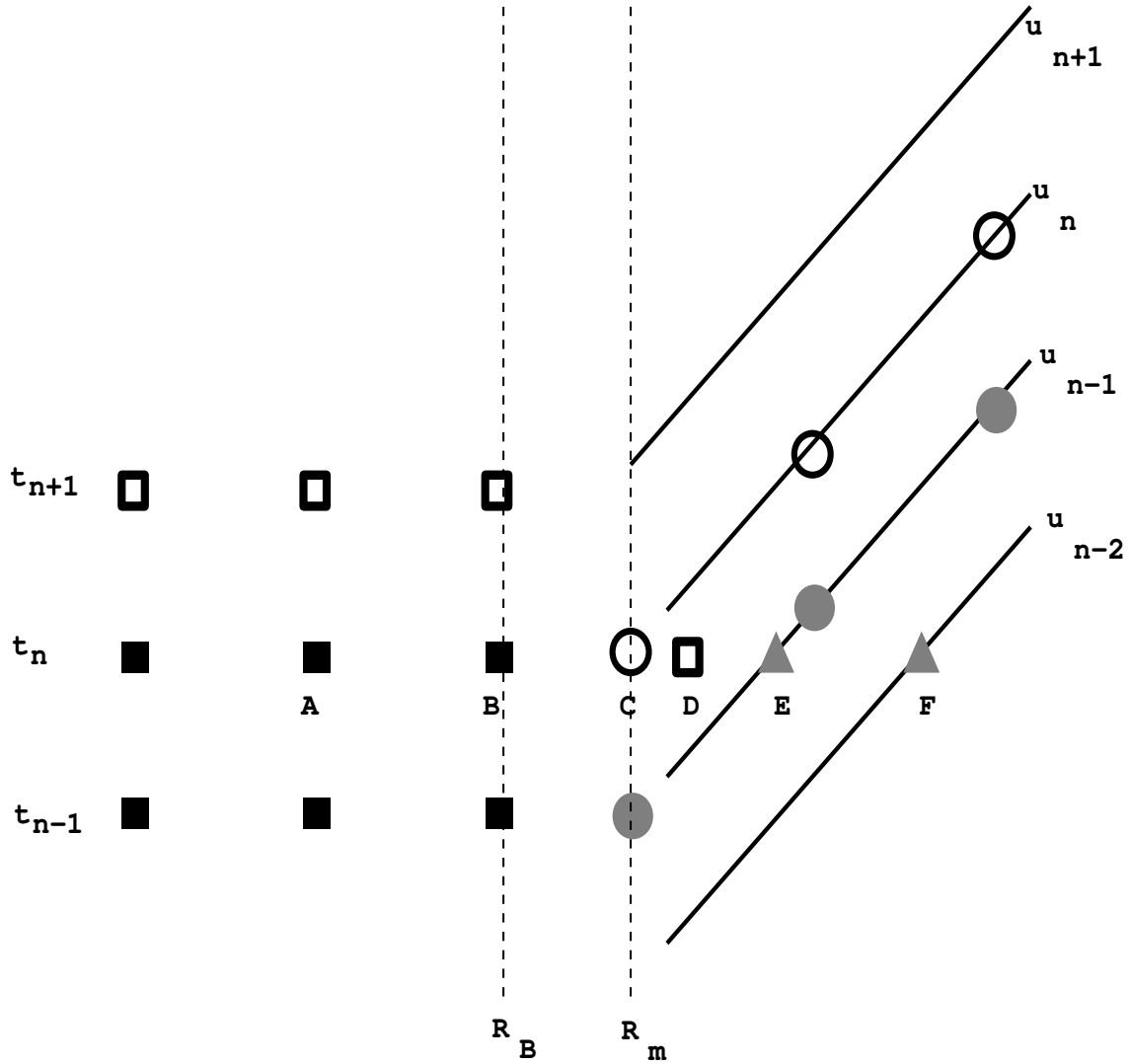


FIG. 4. Cauchy grid points are indicated by squares and characteristic grid points by circles. The triangles indicate points E and F where the time level t_n intersects the retarded time levels u_{n-1} and u_{n-2} . Initial data are given at the shaded points. Evolution proceeds iteratively by determining field values at the unshaded points. The matching scheme provides boundary values at C ($r = R_m$) and D ($r = R_B + \Delta r$) for the characteristic and Cauchy grids, respectively.

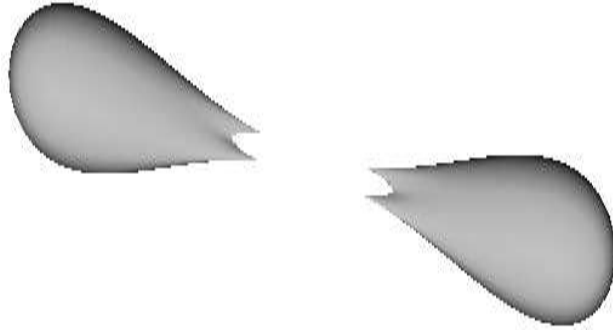


FIG. 5. Prelude to a generic collision of black holes. As they approach, the initially spherical black holes are tidally distorted.

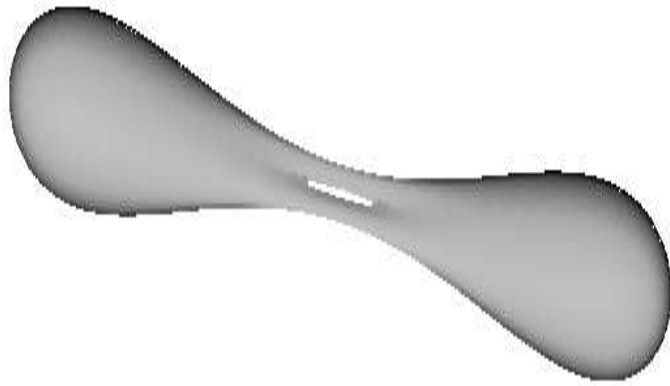


FIG. 6. Temporarily toroidal black hole produced by the merger of two black holes. The hole in the torus soon closes up to form a peanut shaped black hole, which then expands into a spherical shape.